South African Journal of Botany 114 (2018) 150–162

Contents lists available at ScienceDirect

South African Journal of Botany

journal homepage: www.elsevier.com/locate/sajb

Cratoxylum formosum ssp. *pruniflorum* activates the TRAIL death receptor complex and inhibits topoisomerase I

A. Nonpunya [a], B. Sethabouppha [b], S. Rufini [c], N. Weerapreeyakul [d,*]

[a] Research and Development in Pharmaceuticals Program, Graduate School, Khon Kaen University, Khon Kaen 40002, Thailand
[b] Faculty of Pharmaceutical Sciences, Ubon Ratchathani University, Warinchamrab, Ubon Ratchathani 34190, Thailand
[c] University of Rome Tor Vergata, Via della ricerca scientifica, Rome 00133, Italy
[d] Faculty of Pharmaceutical Sciences, Khon Kaen University, Khon Kaen 40002, Thailand

ARTICLE INFO

Article history:
Received 1 August 2017
Received in revised form 30 October 2017
Accepted 3 November 2017
Available online xxxx

Edited by L Rárová

Keywords:
Cratoxylum formosum ssp. *pruniflorum*
Apoptosis
FTIR
Death receptor pathway
Intrinsic pathway
Topoisomerase inhibitor

ABSTRACT

Six species of *Cratoxylum* are found in Thailand. Whether the *Cratoxylum formosum* ssp. *pruniflorum* (CFP) has anticancer properties requires investigation. CFP exhibited cytotoxicity against hepatocellular carcinoma HepG2 cells. Based on FTIR microspectroscopy, CFP raised the respective lipid and nucleic acid content and β-pleated sheet in HepG2 cells, suggesting a change in the secondary protein structure. CFP induced apoptosis by increasing the activities of various caspases. Overexpression of TRAILR2 indicated the extrinsic pathway while expression of Bax/Bcl-2 ratio indicated the intrinsic pathway and decreased expression of Bid indicated cross-talk between the two. CFP alkylated the DNA and caused DNA damage, which may be the initial step in the intrinsic pathway. CFP indirectly and directly inhibited Top IB enzyme activity and decreased PARP—the protein-related DNA repair process. CFP could, thus, protect the resistance mechanism of cancer by reversing the effect of Top as confirmed by apoptosis induction in the resistant HepG2 cells. The phytochemical analysis suggested that the compounds playing an important role in the anticancer activity of CFP are a group of xanthones.

1. Introduction

Cratoxylum formosum ssp. *pruniflorum* belongs to the family of Guttiferae, which is found throughout Southeast Asia (Boonnak et al., 2006). Six species are found in Thailand (Boonnak et al., 2006). Two subspecies (ssp.) of *C. formosum*—ssp. *formosum* and ssp. *pruniflorum*—are mistakenly mismatched due to their similarity and close Thai names. Ssp. *formosum* (CFF) is called Tiew khao in Thai, while spp. *pruniflorum* (CFP) is called Tiew kon. The more edible, *Cratoxylum* is ssp. *formosum* (CFF), is eaten as a side dish due to its sour taste. The edible part of CFF comprises fresh young leaves and these are commonly available in local markets in northeastern Thailand. By contrast, CFP is not so palatable because it has tiny hairy leaves and is astringent.

Cratoxylum genus has long been used in traditional medicine for relieving several diseases (Boonnak et al., 2006). Traditional use of bark or leaves of CFF is as a tonic, stomachic, diuretic (Grosvenor et al., 1995a, 1995b; Waiyaput et al., 2012), diarrhea, flatulence (Anderson, 1986), food poisoning, internal bleeding (Grosvenor et al., 1995a, 1995b) while the roots and leaves are used for relieving liver cirrhosis (Waiyaput et al., 2012; Issara-Amphorn and T-Thienprasert, 2014). The leaves of CFP are used for heat and thirst quenching, detoxifying, preventing obesity, reducing blood fat, and lowering blood pressure (Xiong et al., 2014). In addition, CFP has long been used to prepare infusions (viz., "Ku Ding tea") by Southern and Southwestern Chinese despite its bitter taste (Xiong et al., 2014).

Several biological activities of both subspecies have been reported but taxonomic authentication was not always provided. CFF was reported to possess anti-oxidant activity (Maisuthisakul et al., 2006; Kukongviriyapan et al., 2007; Waiyaput et al., 2012), anti-bacterial (Boonsri et al., 2006), and cytotoxic effect on MCF-7 (breast adenocarcinoma), HeLa and Caski (human cervical cancer) (Kuete et al., 2011), KB (human oral cancer), and HT-29 (colon cancer) (Boonsri et al., 2006). Ethanolic extract of CFF leaves showed cytotoxicity against HepG2 hepatocellular carcinoma cells (Prayong et al., 2008), a gastroprotective effect (Sripanidkulchai et al., 2010), and an inhibitory effect on HBV

Abbreviations: Bax, Bcl-2 associated X protein; Bcl-2, B cells lymphoma-2 protein; Bid, Bcl-2 homology interacting domain death against; CFP, *Cratoxylum formosum* (Jack.) Dyer ssp. *pruniflorum* (Kurz) Gogel; DISC, Death inducing signaling complex; FADD, Fas associated death domain; FTIR, Fourier transform infrared; GC–MS, Gas chromatography–mass spectrometry; HCC, Human hepatocellular carcinoma; HepG2, Hepatocellular carcinoma cell lines; PARP, Poly-ADP ribose polymerase; PVDF, Polyvinylidene difluoride; SDS-PAGE, Sodium dodecyl sulfate-polyacrylamide gel electrophoresis; tBid, Truncated Bid; Top IB, Topoisomerase IB enzyme; TRAIL-R2, Tumor necrosis factor related apoptosis inducing ligand -receptor 2; Vero, African green monkey kidney cells.

* Corresponding author at: Division of Pharmaceutical Chemistry, Faculty of Pharmaceutical Sciences, 123 Mittrapap Road, Amphoe Muang, Khon Kaen University, Khon Kaen 40002, Thailand.
E-mail address: natthida@kku.ac.th (N. Weerapreeyakul).

https://doi.org/10.1016/j.sajb.2017.11.003
0254-6299/

replication (Waiyaput et al., 2012). Xanthone V1 from CFF showed cytotoxicity against the Hela, Caski, MCF-7, PF-382 cell lines, were anti-angiogenesis, and arrested the cell cycle in the S phase (Kuete et al., 2011). Meanwhile, CFP was reported to have an anti-microbial effect (Boonnak et al., 2006; Kuvatanasuchati et al., 2011). The combination of two pure compounds isolated from the roots of CFP—macluraxanthone and garcinone B—showed a synergistic effect against both gram positive and gram negative bacteria (Boonnak et al., 2010). Compounds separated from CFP stem—i.e., pruniflorone Q, pruniflorone R, 1,7-dihydroxy-8-methoxyxanthone, 1,4,7-trihydroxy-8-methoxyxanthone, 1,7-dihydroxy-4-methoxyxanthone, 1,3,6-trihydroxy-7-methoxyxanthone, dulcisxanthone B, cudratricusxanthone E, cochinchinone B—were reported to inhibit the retinoid receptor RXR, which is related to the transcription factor associated with gene expression (Duan et al., 2010, 2011). In addition, xanthones from CFP leaves (i.e., toxyloxanthone B and vismione D) showed an anti-inflammatory effect through inhibition of NO production (Boonnak et al., 2014; Xiong et al., 2014) while toxyloxanthone B showed a significant neuroprotective effect against β-amyloid in neuroblastoma cells (Xiong et al., 2014). Hydroethanolic (50%) extract of CFP twig delayed amyloid-β induced paralysis in *C. elegans*, providing useful information for developing an anti-Alzheimer candidate (Keowkase and Weerapreeyakul, 2016).

According to the literature review, anticancer activity of both CFF and CFP has been reported. Our group previously reported the anticancer potential of 50% hydroethanolic extract from both CFF leaves (Prayong et al., 2008) and CFP twigs (Nonpunya et al., 2014). A polar solvent was selected for the extraction to emulate a decoction. CFP extract induced apoptosis in U937 leukemia cells as determined by FTIR microspectroscopy (Machana et al., 2012) and induced caspases-mediated apoptosis in HepG2 cells (Nonpunya et al., 2014). CFP extract has been shown to be a good candidate for anticancer activity in HepG2 cells; however, the detailed cellular effect of CFP on these cancer cells is lacking. Hepatocellular carcinoma (HCC) was the focus of the current study due to its high mortality rate among people in the Asia-Pacific region (Zhu et al., 2016). HCC patients were reported to have a poor prognosis due to a resistance mechanism by HCC against anticancer drugs and the limited choice of treatments because of the often advanced stage of the disease at diagnosis (Issara-Amphorn and T-Thienprasert, 2014). An alternative treatment (or the development of a new source of anticancer agents) was therefore needed. In the current study, we aimed to investigate the mechanisms of anticancer action against HCC. One useful technique for monitoring biological alterations and predicting the structure of molecules (such as proteins) is Fourier transformation infrared (FTIR) microspectroscopy (Srisayam et al., 2014; Junhom et al., 2016; Siriwarin and Weerapreeyakul, 2016). FTIR microspectroscopy was used to evaluate the biomolecular changes related to the IR spectra absorption in CFP extract-treated HepG2 cells.

2. Materials and methods

2.1. Materials

Human hepatocellular carcinoma cells (HepG2) (ATCC#8065), and African green monkey kidney (Vero) (ATCC#CCL-81) were purchased from American Type Culture Collection (ATCC) (Manassas, VA, USA). The reagents used in the cell culture were biological grade and obtained from GIBCO, Invitrogen Corporation (Grand Island, NY, USA). Neutral red, melphalan, and 5-FU were purchased from Sigma Aldrich Co. (St. Louis, MO, USA). The BCA assay kit was obtained from Pierce Biotechnology (Rockford, IL, USA). The primary antibodies—Bax, Bcl-2, TRAILR, PARP, Bid and β-actin—were purchased from Santa Cruz Biotechnology (Dallas, Texas, USA). The goat anti-mouse IgG1 heavy chain (horseradish peroxidase) was purchased from Abcam (Cambridge, UK). The protease inhibitor cocktail was purchased from Amresco® (solon, OH, USA). The Apoalert™ caspase fluorescent assay kit was purchased from Clontech Laboratories, Inc. (Mountain View, CA, USA). The enhanced chemiluminescence (ECL) reagent was bought from GE Healthcare UK Limited (Buckinghamshire, UK). FITC-conjugated annexin V and Propidium iodide (PI) were purchased from eBioscience (San Diego, CA, USA). The purified topoisomerase IB (Top IB) enzyme was provided by Professor Alessandro Desideri, Department of Molecular Biology, Faculty of Science, University of Rome Tor Vergata, Italy. The reagents for the NP-40 buffer (NaCl, TritonX, Tris and EDTA) were purchased from Sigma-Aldrich Chemie GmbH (Munich, Germany).

2.2. Plant extraction

Twigs of CFP were collected in northeastern Thailand in 2013. The herbarium collection (voucher specimen TTOC-SK-862) was kept at the Faculty of Pharmaceutical Sciences, Khon Kaen University, Thailand. A 50% hydro-ethanolic crude extract was prepared as per Nonpunya et al. (2014).

2.3. Phytochemical analysis

The major phytoconstituents—tannins, xanthones, terpenoids, saponins, steroids, alkaloids, and glycosides—in 0.05 g of CFP extract were identified as per previous reports with some modification (Ukoha et al., 2011; Manosroi et al., 2012; Gangwar et al., 2014). Briefly, the CFP extract (0.05 g) was dissolved in 2 mL of ethanol, incubated in a water bath (40 °C) for 10 min, centrifuged at 268.3 × *g* for 10 min, and the supernatant collected. For tannin, 2 mL of 15% $FeCl_3$ was added and a dark green or blue-black precipitate indicated the presence of tannin. Xanthones were indicated by a yellow precipitate, after adding 100 μL of 5% KOH to the supernatant (Manosroi et al., 2012). For terpenoids, CFP extract was dissolved in 2 mL of chloroform and dried in a water bath. After that, 2 mL of concentrated sulfuric acid was added and heated for another 2 min. A dark-gray color indicated the presence of terpenoids (Ukoha et al., 2011). While steroids were indicated after dropping concentrated sulfuric acid sidewise into CFP dissolved in chloroform. The red formation in the chloroform layer indicated the presence of steroids (Gangwar et al., 2014). Saponins were indicated by permanent foam at RT after CFP was dissolved in deionized water for 1 h and shaken vigorously for 30 min (Ukoha et al., 2011). CFP extract was dissolved in 1 mL of methanol and filtered. The supernatant was kept and 2 mL of 1% HCl added, followed by 1 drop of Dragendorff's reagent (potassium bismuth iodide). A reddish-brown precipitate with turbidity indicated the presence of alkaloids (Ukoha et al., 2011). Glycosides were indicated by Fehling reagent mixture (Fehling A: Fehling B = 1:1), as per Manosroi et al. (2012); and Ukoha et al. (2011). Fehling's solution A was a mixture of 3.5 g of copper II sulfate in 50 mL deionized water; while Fehling's solution B comprised 5 g sodium hydroxide, 17.5 g potassium sodium tartrate and 50 mL of deionized water. The CFP extract was dissolved in 1 mL of deionized water then heated with 1 mL of Fehling reagent mixture for 10 min. A brick-red precipitate indicated the presence of reducing sugar in the glycosides.

2.4. Standardization and phytochemicals analysis of 50% hydroethanolic extract of CFP extract

GC–MS analysis was performed as previously described (Weerapreeyakul et al., 2016) on an Agilent 6890 N gas chromatograph (Agilent Technologies, Shanghai, China) coupled to an Agilent 5973 N mass selective detector (Agilent Technologies, Shanghai, USA) to determine the extract composition for further standardization. Capillary GC analysis was performed using a DB-5 ms (3 m × 0.25 mm id, 0.25 μm) capillary column from Agilent Technologies (J&W Scientific, Folsom, CA, USA). Helium was used as the carrier gas. The column initially flowed at 80 °C for 6 min at a rate of 2 mL/min and an average velocity of 52 cm/s. The temperature was increased to 280 °C (at a rate of 5 °C/min) for 24 min. The total run-time was 70 min. The injector temperature was maintained at 250 °C and the injection volume was 2.0 μL in the splitless

mode. The interface temperature was held at 280 °C. Mass spectra were scanned from *m/z* 50.0 to *m/z* 500.0 at a rate of 1.5 scans/s with a threshold of 150. The electron impact ionization energy was 70 eV. The chemical components of the crude extracts were identified from the chromatograms and mass spectra using the Wiley 7 N.l database (Agilent Technologies, Santa Clara, CA, USA).

2.5. Cell cultures

The human hepatocellular carcinoma (HepG2) cell line, cisplatin-resistant HepG2 cells, and normal African green monkey kidney epithelial (Vero) cell lines were cultured in DMEM. The medium was supplemented with 10% FBS, 100 units/mL penicillin, and 100 μg/mL of streptomycin. The cells were cultured in an incubator (Thermo Fisher Scientific, Waltham, MA, USA) at 37 °C under a humidified atmosphere containing 5% CO_2.

2.6. Cytotoxicity effect

The cytotoxic activity of the CFP extract in hepatocellular carcinoma (HepG2) and noncancerous (Vero) cell lines were evaluated using neutral red assay as per Nonpunya et al. (2014). Briefly, cells (4×10^5 cells/mL) were seeded in 96-well plates for 24 h then treated with various concentrations of CFP extract (10, 25, 50, 100, 250, and 500 μg/mL) and melphalan (10, 25, 50, 100, 250, and 500 μg/mL) for 24 h. After 24 h, the cells were stained with neutral red dye (to a final concentration of 50 μg/mL) and incubated at 37 °C for another 2 h. The neutral red stained-viable cells were lysed by 0.33% hydrochloric acid in isopropanol and detected using colorimetry. Absorbance (Abs) was measured at 520 nm and 650 nm (reference wavelength) using a UV-microplate reader (Tecan, Switzerland). The concentration needed to inhibit the cell viability by one-half (or an IC_{50} value) was calculated. The selectivity index (SI) was calculated from the IC_{50} of the CFP extract in the Vero cells over the HepG2 cancer cells to determine the cytotoxic selectivity of the CFP extract.

2.7. FTIR microspectroscopy

2.7.1. Cell sample preparation

HepG2 cells (1×10^6 cell/mL) were treated with CFP extract at 1 × IC_{50} and 2 × IC_{50}) (60 or 120 μg/mL, respectively) or melphalan at 2 × IC_{50} concentrations (80 μg/mL) for 24 h in 24-well plates. Then the cells were harvested and gently washed with 0.9% NaCl before being deposited onto Low-e Microscope slides (MirrIR, Kevlev Technologies, Chesterland, OH, USA). Cells were dried under vacuum for 30 min, rinsed for a few seconds with a small amount of distilled water followed by vacuum drying. This step was repeated for complete removal of the salt. The free-salt cells were kept in a desiccator for future use.

2.7.2. Cellular effect of CFP on biomolecular changes

Biomolecular alteration was determined by FTIR microspectroscopy after the cells were treated with CFP extract or melphalan for 24 h. The HepG2 Cell samples were analyzed in the transfection mode, using a conventional internal IR source in a Bruker Vertex 70 spectrometer connected to a Brucker Hyperion 2000 microscope (Bruker Optics Inc., Ettlingen, Germany). The microscope was equipped with a nitrogen-cooled MCT (HgCdTe) detector (area 250 × 250 μm^2). IR signals were acquired from 60 to 70 cells comprising 68 × 68 μm^2 spot areas, mapped within most homologous zones. Sixty-four scans (20 kHz velocity and 4 cm^{-1} spectral resolution) were performed within the 4000–6000 cm^{-1} spectral interval in order to obtain an average spectrum with an appropriate signal-to-noise ratio. Spectral acquisition and instrument controls were performed using OPUS 6.5 software (Bruker Optics Inc., Ettlingen, Germany).

Principal Component Analysis (PCA) was performed using variables within the spectral range of 3000–2800 cm^{-1} and 1790–900 cm^{-1}. Unscrambler software (version 9.7, CAMO Software AS, Oslo, Norway) was used for discrimination of any significant variation between the data sets. Variability related to the variable baseline, different sample thickness, and scattering artifacts were minimized by normalization with extended multiplicative signal correction (EMSC) after being processed, by taking the second derivative per the Savitzky–Golay algorithm (9 points of smoothing allowing minimization of the effects of variable baselines). Six PCs were selected for analysis of the biomolecular alteration for between-groups comparisons. A loading plot was used to display variations within each data set. Curve-fitting analysis was performed using OPUS 6.5 software. The amide I region (1710–1590 cm^{-1}) was selected for differentiating the secondary structure of proteins. The Gaussian and Laurence algorithms were used for the curve-fitting.

2.8. Apoptosis inducing effect

2.8.1. Flow cytometry analysis

The Annexin V-FITC and PI apoptosis assay kit was used to distinguish early and late stage apoptotic cell death from necrosis by standard FACS assay. Briefly, cells (1×10^6 cell/mL) were treated in 24-well plates for 24 h with melphalan (80 μg/mL) or CFP extract (60 or 120 μg/mL, respectively). The cells were detached with 0.25% trypsin–EDTA, washed with ice cold 1 X PBS, and pelletized by centrifugation at 700 × *g* for 5 min. The cells were then re-suspended with 95 mL of binding buffer (HEPES buffered saline supplemented with 25 mM $CaCl_2$) followed by staining with Annexin V-FITC (5 mL) for 15 min (dark condition). Then cells were stained with 100 mL of PI solution (5 μL of PI in 95 μL of binding buffer) and incubated for another 15 min in the dark at RT. The staining cells were then subjected to flow cytometry (FCM) (BD FACSCanto II, BD Biosciences, San Jose, CA, USA). The viable, apoptotic, and necrotic cells were detected by BD FACSDiva software (BD Biosciences, San Jose, CA, USA).

2.8.2. Caspases enzyme activity

Caspase activities were measured using the Apoalert™ caspase fluorescent assay kits, according to the instructions provided. Briefly, after cells (4×10^5 cells/mL in 96-well plate) were treated with 60 μg/mL of CFP extract for 24 h, cells were harvested and lysed by 2X ice cold lysis buffer (from the Kit) for 30 min. Then cells were pelletized by centrifugation at 32,869 × *g* for 10 min, 4 °C. The supernatant was kept on ice until used. According to the company assay protocol, the microplates were pre-coated with specific substrate of each caspase linked to the fluorogenic dye 7-amino-4-metyl coumarin (AMC). One hundred microliters of reaction mixture were added (50 μL of supernatant and 50 μL 2X reaction buffer/DTT mix) and the mixture incubated for another 2 h. The fluorescence of AMC was detected using a fluorescent microplate reader (excitation at 380 nm and emission at 480 nm). The data were expressed as means ± SD of three determinations.

2.8.3. Expression of apoptosis related proteins

Western blot analysis was performed as per Junhom et al. (2016) with some modifications. Briefly, after cells (3×10^5 cells/mL in cell culture dish) were treated with various concentrations of CFP extract, they were washed with ice cold 1X PBS and pelletized by centrifugation at 700 × *g* for 5 min. Cells were then lysed with NP-40 lysis buffer [150 mM NaCl, 1%TritonX, 50 mM Tris (pH 8), 5 mM EDTA] supplemented with 1X protease inhibitor cocktail for 1 h at −20 °C, followed by centrifugation at 32,869 × *g* for another 15 min at 4 °C. The supernatant was collected and the protein quantified using a BCA assay kit. Equal amounts of protein (60 μg in 5 μL) were prepared individually by mixing a sample with 5X loading buffer (1 μL) [1 M Tris (pH 6.8), sodium dodecyl sulfate, bromophenol blue, dithiothreitol] followed by heating at 100 °C for 5 min. Afterwards the protein was separated by 10% SDS-PAGE. The protein was then transferred to a polyvinylidene difluoride membrane and blocked with a non-specific protein with 5% blocking buffer [5% nonfat dry milk in TBST, 50 mM Tris/HCl pH 7.7, 150 mM NaCl,

0.1% Tween-20] for 2 h, 25 °C. The membrane was incubated with primary antibodies [i.e. Bax (1:200), Bcl-2 (1:500), Bid (1:200), TRAILR-2 (1:500), PARP (1:2000) and β-actin (1:1000)], which were diluted in 5% non-fat dry milk/TBS-T overnight at 4 °C. The membrane was then washed with TBS-t buffer 3X followed by incubation with secondary anti-body [goat anti-mouse IgG linked to peroxidase; HRP-conjugated goat anti-mouse IgG (1:1000)] for another 2 h, 25 °C. Then the membrane was washed again with TBS-t; before adding the enhanced chemiluminescence (ECL) reagent for detection of the protein expression band.

2.9. Alkylating activity assay

To determine the anticancer mechanism related to DNA damage, the CFP extract was examined for DNA alkylation activity in vitro. Melphalan—the standard alkylating drug which causes DNA strand break and DNA damage—was used as a positive control, while 5-fluorouracil (5-FU), non-alkylating anticancer drug was used as the negative control. The pyridine ring of nitrogen in 4-(4′-nitrobenzyl) pyridine (NBP)—a DNA base mimic—was used to test the alkylating ability of the test compounds in vitro. The NBP assay was conducted with minor modifications (Budzisz et al., 2003). Briefly, the CFP extract (500 μg/mL) or 5-FU (8 μg/mL) or melphalan (80 μg/mL) were added to the buffer solution (pH 4.0) containing NBP and incubated at 70 °C for 30 min. The mixture solution was added (in a 1:3 ratio) to test plates containing a cold mixture solution of absolute ethanol and 0.1 N NaOH. The blue color of the alkylated product was measured for absorbance using a UV–Vis spectrophotometer (UV-1700 PharmaSpec, Shimadzu, Tokyo, Japan) at 600 nm. The alkylating capability was determined from the absorbance value (Abs) and classified into 3 classes (Budzisz et al., 2003); including: (1) very high alkylating activity (Abs > 0.50); (2) high alkylating activity (0.15 ≥ Abs ≥ 0.50); and, (3) low alkylating activity (Abs < 0.15). The percentage alkylating activity of the CFP extract was compared to positive and negative controls.

2.10. DNA topoisomerase IB enzyme activity

The relaxation assay was conducted according to previous report with some modification (Jahan et al., 2013). The experiments were separated into 2 assays.

First, the investigation of the indirect effect of CFP extract on DNA relaxation via cellular effect stimulation. Briefly, after HepG2 cells were treated with 120 μg/mL CFP extract for 1 h, the cells were washed 3X with ice cold 1X PBS and pelletized by centrifugation at 700 × *g* for 5 min. The cells were then lysed with RIPA buffer (150 mM NaCl, 50 mM Tris (pH 8), 1% NP-40 (150 mM NaCl, 1% TritonX and 50 mM Tris pH 8.0 and 5 mM EDTA), 12 mM sodium deoxycholate, 0.1% SDS) supplemented with 1X protease inhibitor cocktail for 1 h at −20 °C followed by centrifugation at 32,869 × *g* for another 15 min at 4 °C. The supernatant was collected and the protein quantified per Lowry's method (Lowry et al., 1951). Equal amounts of protein (60 μg) were prepared and incubated with various amounts of purified Top IB enzyme followed by the addition of 30 μL reaction volume, comprising 0.5 μg of negatively supercoiled pBlue Script KS II (+) DNA and reaction buffer (20 mM Tris–HCl, 0.1 mM Na_2EDTA, 5 mM $MgCl_2$, 50 μg/mL acetylated BSA, and 120 mM KCl, pH 7.5).

Second, the direct effect of CFP extract against the Top IB enzyme was determined. The CFP extract was incubated with Top IB purified enzyme followed by addition of the reaction mixture. The reaction was stopped by 0.5% SDS (final concentration) after incubating all of the samples for 1 h at 37 °C. The DNA relaxation was assessed by horizontal gel electrophoresis (1% agarose gel in 50 mM Tris, 45 mM boric acid, 1 mM EDTA) 22 V, overnight. Then the gel was stained with ethidium bromide (5 μg/mL) for 15 min and de-stained with water 3X before being photographed under UV illumination (U:genius 3, Syngene, MD, USA).

2.11. Cancer cell sensitivity in resistant HepG2 cells

Since increasing doses of chemotherapeutic agents are normally required in order to eliminate resistant cancer cells, it will lead to high toxicity, resulting in limitation of the cancer treatment. To evaluate the sensitivity of the CFP extract in resistant HepG2 cancer cells, the following parameters were measured using 500 μg/mL of CFP extract: (1) the cytotoxicity via NR assay, (2) the apoptosis-inducing effect by flow cytometry, and (3) the protein expression (Bax, Bcl-2) western blot analysis against the resistant HepG2 cells (3.5 resistance fold higher than the parental HepG2 cells). This resistant HepG2 cell model was produced as previous report (Junhom et al., 2016).

2.12. Statistical analyses

The data were presented as means ± standard deviation (SD) (n = 3). Differences among multiple-group comparisons were evaluated using one-way ANOVA followed by a Tukey's honest significant difference using SPSS Windows version 11.5 (SPSS, USA). Evaluation with a two-tailed Student's *t*-test was also performed for two-group comparisons. Values of $P < 0.05$ were considered statistically significant.

3. Results

3.1. Phytochemical analysis

The different phytochemicals in the 50% CFP extract are presented in Table 1. The rank from high to low content of identified compounds in the CFP extract was xanthones, terpenoids, tannin, saponin, alkaloids, and reducing sugars. A very deep color was observed in the xanthones test, which indicated a higher level of xanthones than any other compound. Quantitative analysis is required before xanthone compounds can be identified.

3.2. Gas chromatography and mass spectrometry (GC–MS) of CFP 50% hydroethanolic extracts

In order to confirm the presence of other compounds, GC–MS was adopted and the identification of the constituents was compared with the library based on the % similarity higher than 90%. The identified compounds are presented in Table 2. Most of the CFP extracts contained fatty acids (i.e., oleic acid and palmitic acid) as well as pyrocatechol and syringol. Although the high temperature from the GC–MS analysis led to degradation of some compounds, the GC–MS profile may be useful as a fingerprint of the extract for future standardization.

3.3. Cytotoxicity

Fig. 1 illustrates that the CFP extract possessed a non-significantly different cytotoxic effect compared to melphalan. The respective IC_{50} value of the CFP extract and melphalan was 55.9 ± 10.6 μg/mL and 37.7 ± 9.8 μg/mL. Lower cytotoxicity (20%) of the CFP extract in Vero normal cells was observed even when the concentration was increased to 500 μg/mL. Thus, CFP showed very low cytotoxicity against Vero cells with an IC_{50} more than 500 μg/mL while melphalan showed an IC_{50} of 59.9 ± 3.2 μg/mL. The CFP extract exerted a highly selective toxicity to the HepG2 cells over against the noncancerous Vero cells (~9-fold higher) (SI = 8.9), while melphalan possessed an SI of 1.6. In order to define the anticancer potential of the CFP extract, the apoptotic-targeting mechanism was further determined.

3.4. Cellular biomolecular alteration

FTIR microspectroscopy is a useful technique for determining molecular structures, which is accomplished by measuring the vibration of functional groups of biomolecules. Infrared radiation is absorbed by

Table 1
Phytochemical analysis of CFP extract.

Plant	Tannin	Xanthones	Terpenoids	Saponin	Steroids	Alkaloids	Reducing sugar
CFP	+++	+++++	++++	++	–	+	+

Note: – = indicates absence of phytochemicals, + = indicates presence of phytochemicals, ++ = indicates small presence; +++ = indicates moderate presence; ++++ = indicates high presence and +++++ = indicates highest presence.

cells due to covalent bond vibration inside cellular biomolecules. The degree of infrared absorbance is according to the nature of covalent bond and the strength of any intermolecular interactions. To illustrate the level of biochemical changes, a histogram (Fig. 2A) was generated from the mean integrated areas of primary spectra for lipid (3000–2800 cm^{-1}), protein (1700–1500 cm^{-1}), carbohydrate and nucleic acid regions (1300–900 cm^{-1}). The lipid and nucleic acid components in HepG2 cells treated with melphalan and $1 \times IC_{50}$ and $2 \times IC_{50}$ of CFP extracts were significantly increased when compared to the control group ($P < 0.05$). CFP had a HepG2 cellular effect in a non-concentration dependent manner.

Principle component analysis (PCA) provides an interpretable overview of the information contained in a multidimensional data table in which rows are the spectra of HepG2 cells and the columns the variables (wave numbers within selected intervals). To more precisely compare the original spectral range, the spectra were processed by taking a second derivative, which better resolved the overlapping peaks of the original spectra. PCA was performed on the second derivative FTIR spectra to discriminate different cell groups (Fig. 2B). The PCA analyzed the scattering of the spectral datasets acquired from the 4 different cell groups (viz., (1) the untreated HepG2 cells; (2) the HepG2 cells treated with melphalan; (3) 60 μg/mL; and, (4) 120 μg/mL CFP extract). These 4 clusters were clearly visualized in two-dimensional score plots-PC1 vs PC-2 from the PCA modeling (Fig. 2B). The PCA results show that the clusters of untreated HepG2 cells were distinctively separated from all the clusters of cells treated with melphalan (i.e., 60 μg/mL and 120 μg/mL of CFP extract, and PC1 (52%)). The spectra of cells treated with 60 μg/mL CFP extract were well-separated from the spectra of cells treated with 120 μg/mL CFP extract and melphalan along PC2 (28%). These results indicated that the spectral clusters of cells treated with melphalan and 120 μg/mL CFP extract possessed a similar pattern of biochemical alterations of the FTIR spectra.

Analyses of the PCA loading plots (Fig. 2C) were used to determine the regions of the second derivative FTIR spectra that most contributed to the clustering. The results obtained from loading plot indicate the biomolecular region responsible for the changes in HepG2 cells after treatment. Significant separation between the clusters of control cells and cells treated with CFP at $1 \times IC_{50}$ (60 μg/mL) was observed on PC1 (Fig. 2B). This clustering showed a high negative value for PC1 loading at 2920 and 2850 cm^{-1} (C—H stretching of lipids) (Fig. 2C) and a high positive value for spectra at 1650 cm^{-1} (α-helix protein structure) and 1540 cm^{-1} (i.e., deformity of the protein at the amide II of the N—H bending and C—N stretching). This indicates that cells treated with 60 μg/mL CFP extract resulted in increasing lipid content in the HepG2 cells compared to the controls (untreated cells). The respective α-helix protein structure peak (1650 cm^{-1}) and deformity of the protein at the amide II band (1540 cm^{-1}) of the control was higher than that of HepG2 cells treated with both concentrations of CFP and melphalan.

When observed in the PC2 loading plot, the cluster of cells in the control and cells treated with 60 μg/mL CFP could be dominantly separated from the cluster of cells treated with 120 μg/mL CFP or 80 μg/mL melphalan. This clustering was heavily loaded so as to have the highest positive value of PC2 loading at 1662 cm^{-1} (β-sheet protein structure). The increasing content of the β-sheet structure was prominent in cells treated with 120 μg/mL CFP and melphalan than those in the control and in cells treated with 60 μg/mL CFP. The negative value of PC2 loading at 2920 cm^{-1} and 2850 cm^{-1} (C—H stretching of lipids) separated the positive score of the spectra of the untreated HepG2 cells and 60 μg/mL CFP-treated HepG2 cells from the negative score of the spectra of the melphalan and 120 μg/mL CFP-treated HepG2 cells. In addition, the negative value of PC2 loading at 1650 cm^{-1} (α-helix protein structure) was higher in the controls and cells treated with 60 μg/mL CFP.

To scrutinize the secondary protein structural change, curve-fitting of the protein region was performed between different spectra of each cell group. The FTIR of the protein regions had two dominant features, namely: the amide I (1700–1590 cm^{-1}) and amide II (1560–1500 cm^{-1}) bands. The spectra in the amide I band region—calculated from the average original spectra—provides the amide I band shape, which comprises 5 components: two β-pleated sheets (1618–1628 and 1635–1641 cm^{-1}); an α-helix secondary structure (1650–1656 cm^{-1}); a β-sheet (1665 and 1670 cm^{-1}); and, turn structures (1680–1685 cm^{-1}) (Fig. 2D). It was observed that the α-helix peak shifted rightward with an increased peak area of the β-pleated sheet shown as a shoulder on the right when compared to the control. Based on PCA analysis and curve fitting, the CFP extract caused an alteration of the α-helix protein structure to a more β-sheet form in the HepG2 cells; similar to that found in cells treated with melphalan.

3.5. Apoptosis induction effect

CFP extract led to HepG2 cell death and effected cellular biochemical changes; thus it was possible to determine that the mode of cell death

Table 2
Table Assigned compounds and mass spectra from GC–MS profile of 50% hydroethanolic extract of CFP at 14.1 mg/500 mL.

Retention time (min)	% of peak height	Mass spectra	Assigned compounds
11.18	4.23	53, 64, 81, 92, 110	Pyrocatechol
12.20	4.13	53, 61, 69, 81, 97, 109, 126	2-Furan carboxaldehyde, 5-(hydroxymethyl)-
15.41	3.21	55, 65, 73, 81, 96, 111, 124, 139, 154	Syringol
24.80	4.45	55, 65, 77, 91, 103,109, 118, 124, 130, 137, 147, 153, 163, 180	2-(2-Oxoethyl)-cis-bicyclo [3.3.0] octane-3,7-dione or 1-pentaleneacetaldehyde
29.53	5.69	60, 73, 83, 97, 115, 129, 143, 157, 171, 185, 199, 213, 227, 256	Palmitic acid
32.65	2.60	55, 67, 81, 95, 109, 123, 136, 150, 164, 263, 280	9,12-Octadecadienoic acid (Z, Z)-
32.76	1.90	55, 69, 83, 97, 111, 123, 137, 151, 166, 180, 193, 207, 222, 235, 249, 264, 280	Oleic acid
33.24	3.29	60, 73, 83, 97, 107, 115, 129, 143, 157, 171, 185, 199, 213, 227, 241, 255, 264, 284	Stearic acid
36.35	10.59	57, 71, 85, 96, 107, 135, 152, 320	4-Trimethylsilyl-3-(1-phenylthiobutyl)pent-3-en-2-one

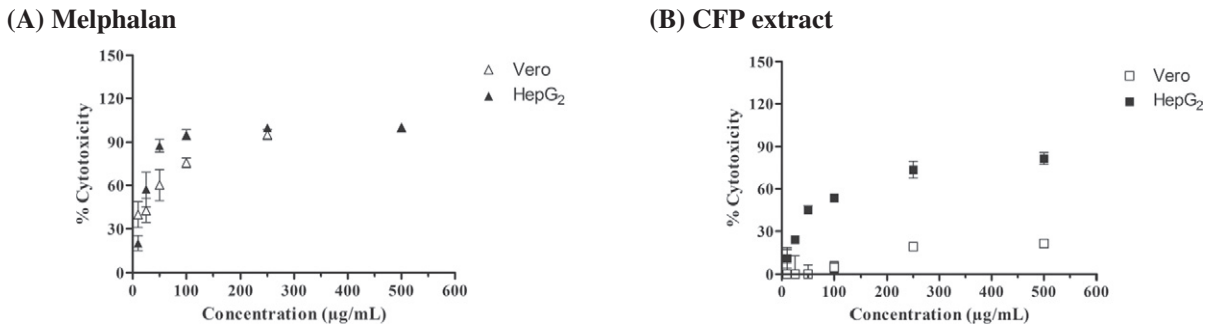

Compounds	IC_{50} (µg/mL)		Selectivity index (SI)
	HepG2	Vero	
CFP extract	55.9±10.6	> 500	8.9
melphalan	37.7±9.8	59.9±3.2	1.6

Fig. 1. Cytotoxicity profiles of **(A)** melphalan (▲) and **(B)** CFP extract (■) against human hepatocellular carcinoma (HepG2) (black symbol) and Vero cells (white symbol). After treatment with various concentrations of CFP and melphalan for 24 h, cytotoxicity was analyzed using neutral red assay. Calculated IC_{50} values and selectivity index were calculated (as shown in the inset). Data are presented as means ± SD from 5 independent experiments.

was apoptosis—i.e., the desirable cell death mode for cancer therapy (McIlwain et al., 2013). Fig. 3A shows that melphalan and CFP extract significantly induced the apoptotic death mode in the HepG2 cells ($P < 0.001$) over against the control. Melphalan resulted in the highest level of apoptosis induction (66.30 ± 4.85%), while CFP significantly induced apoptosis in a concentration-dependent manner ($P < 0.05$) (i.e., a higher % of apoptotic cells at a late stage was found at increased concentrations of CFP extract). Our results show that CFP and melphalan induced only a slight degree of necrotic cell death. Importantly, unwanted necrotic cell death was not increased when increasing CFP extract concentration.

3.6. Caspases activation

Caspase enzymes play an important role in mediated apoptosis; as the pathways of apoptosis could be defined from the activation of caspase activities (Fig. 3B). Executioner caspase 3 is activated when cells die via apoptosis. The activity of caspases 8 and 9 indicate that the pathway of apoptosis induction is via extrinsic and intrinsic pathways, respectively. Fig. 3B shows that activity of all of the caspases was significantly increased ($P < 0.05$) in the HepG2 cells exposed to both CFP extract and melphalan when compared to the control. Increasing caspase activity due to the CFP extract was concentration dependent; indicating that CFP extract induces apoptosis in HepG2 cells via both extrinsic (by caspase 8) and intrinsic pathways (by caspase 9). The current study thus clarifies the relationship of proteins to apoptosis induction pathway.

3.7. Over-expression of pro-apoptotic and anti-apoptotic proteins

The over-expression of proteins related to apoptosis was investigated (i.e., the pro-apoptotic protein Bax and the anti-apoptotic protein Bcl-2, the death receptor TRAILR, Bid, as well as the relationship of DNA repair and poly ADP-ribose polymerase (PARP) (Fig. 4A). After cells were treated with various concentrations of CFP extract (30, 60, 120, and 240 µg/mL) for 24 h, it was found that CFP extract significantly decreased the expression of the anti-apoptotic protein Bcl-2 compared to the control group ($P = 0.001$) (Fig. 4B). The CFP extract at the same concentration significantly increased the Bax/Bcl-2 ratio ($P < 0.05$) and decreased the level of Bcl-2 (Fig. 4C), suggesting an imbalance between Bax over Bcl-2, which occurred via the mitochondrial (intrinsic) pathway.

In the current study, the CFP extract significantly increased TRAILR2 (DR5) expression in a concentration-dependent manner ($P < 0.001$) (Fig. 4D). This result was initially observed at 30 µg/mL of CFP—a lower concentration than the IC_{50} concentration (60 µg/mL). It was confirmed that the CFP extract induced apoptosis via the extrinsic pathway by increasing death receptor TRAILR2 expression followed by activation of caspase 8 activity.

The results shown in Fig. 4E strongly support the crosstalk phenomenon effected by 120 and 240 µg/mL of CFP in HepG2 cells, according to a significant decrease in the Bid protein when compared to the control.

Poly (ADP-ribose) polymerase (PARP) is a key enzyme in transcription, cell cycle regulation, and response to environmental stress (i.e., DNA damage). One function of PARP is DNA repair and relatedly programmed cell death. After HepG2 cells are exposed to CFP extract at various concentrations for 24 h, the expression of full-length PARP (116 KDa) was decreased in a concentration-dependent manner (Fig. 4F). PARP expression was significantly decreased at 240 µg/mL CFP when compared to the control ($P < 0.001$).

3.8. Alkylation in vitro

Alkylation is an effective mode of anticancer-action-targeting via DNA bases. Our results show that CFP extract (absorbance of 1.137) has an alkylating capability in the same category as the positive control drug melphalan (absorbance of 2.768); having a very high alkylating activity (i.e., absorbance >0.50) (Table 3). One anticancer mechanism of CFP extract is via intrinsic apoptosis induction, which is initiated by DNA alkylation, leading to DNA damage.

3.9. Inhibition of topoisomerase IB enzyme

The direct effect of CFP against purified Top IB enzyme was investigated by first fixing the concentration of CFP extract at 60 µg/mL. The amount of Top IB was varied from 0.6, 1.25, 2.5 to 5 µg (Fig. 5A). The results showed that purified Top IB was capable of relaxing the negative supercoiled plasmid DNA at concentrations starting from 1.25 µg, and completely relaxed the supercoiled DNA at 5 µg. The fixed concentration of 60 µg/mL CFP extract had a direct effect on inhibiting purified Top IB activity between 0.6–2.5 µg, resulting in DNA being supercoiled (Fig. 5A). This direct inhibition of Top IB enzyme was not, however, observed at 5 µg purified Top IB due to the high amount of Top IB enzyme under the conditions studied. To confirm the direct inhibition of Top IB activity, the amount of Top IB enzyme was fixed at 2.5 µg while the concentration

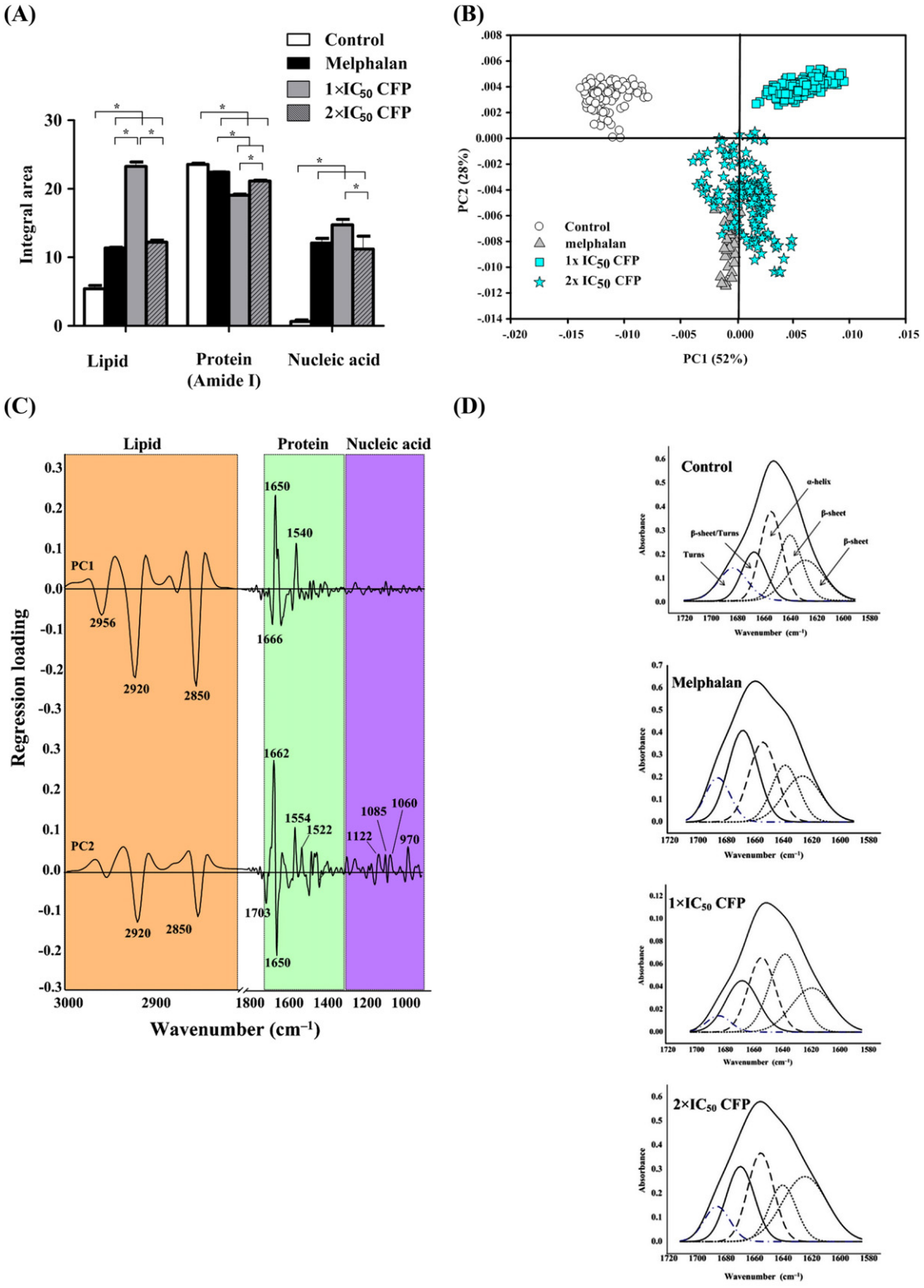

Fig. 2. Histogram **(A)** represents mean integral area for lipid (3000–2800 cm^{-1}), protein (1700–1500 cm^{-1}), carbohydrate and nucleic acid (1300–900 cm^{-1}) of original spectra of 4 different groups of HepG2 cells. *Statistically significant differences in mean integrated area of a given peak region (mean ± SD, N = 3, one-way ANOVA followed by Tukey test, $P < 0.05$). PCA analysis of FTIR spectra (spectral range from 3000 to 900 cm^{-1}). PCA score plots **(B)** of HepG2 cells were calculated from second derivatives spectra from 88, 159, 141 and 90 of standard melphalan (80 μg/mL), CFP extract at 1 × IC_{50} (60 μg/mL) and 2 × IC_{50} (120 μg/mL) and control (untreated group), respectively. PCA score plots exhibited distinct clustering of cells treated with control (○), 80 μg/mL melphalan (△), 60 μg/mL (□) and 120 μg/m of CFP extract (☆), respectively, after 24 h. PCA loading plots **(C)** indicated biomarker difference by discriminating wave numbers over spectral range of cell samples. Curve fitting **(D)** represented by absorbance of amide I band contour with best-fit 50% Loentzian/Gaussian individual component bands for untreated HepG2 (RMS error of 0.0037), HepG2 treated with melphalan (RMS error of 0.0037), HepG2 treated with 1 × IC_{50} (60 μg/mL) and 2 × IC_{50} (120 μg/mL) of CFP (RMS error of 0.0035 and 0.0036, respectively).

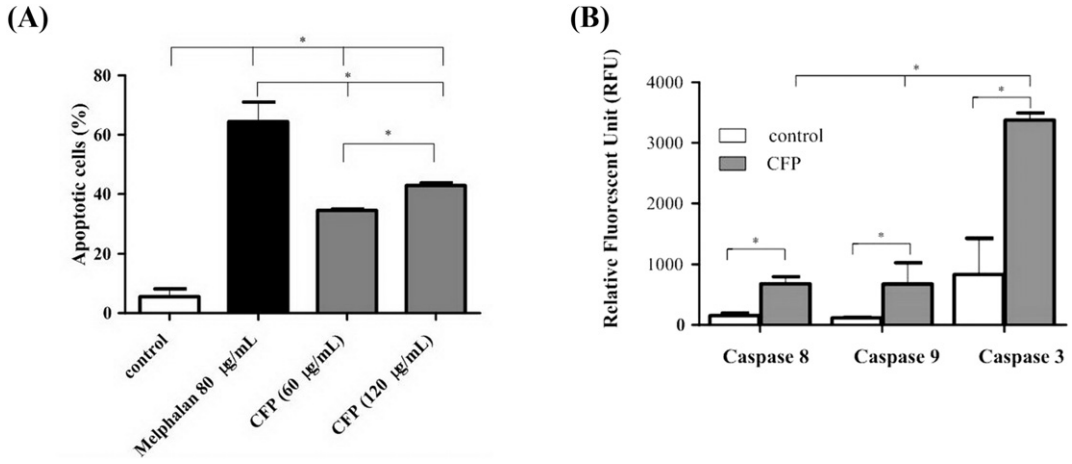

Fig. 3. (A) Percentage of total apoptotic HepG2 cells after treatment with 80 μg/mL melphalan (■), 60 and 120 μg/mL of CFP extract (▨) for 24 h. All data presented as means ± SD from 3 independent experiments. *Significant differences from the control or untreated cells (□), $P < 0.05$. **(B)** Activation of caspases 3, 8, and 9 activities in HepG2 cells treated with 120 μg/mL CFP for 24 h. Results are representatives of triplicate experiments. *Statistically significant differences (mean ± SD, N = 3, one-way ANOVA followed by Tukey test, $P < 0.05$).

of CFP extract varied (0.6, 6, 15, 60, and 120 μg/mL) (Fig. 5B). CFP extract started to inhibit 2.5 μg Top IB enzyme at 60 μg/mL (Fig. 5B).

CFP extract showed cellular biochemical changes to the HepG2 cells, based on FTIR microspectroscopy; hence, the indirect effect of CFP was determined vis-à-vis DNA relaxation by Top IB through the cellular effect. The HepG2 cells were added with the negative supercoiled plasmid DNA and purified Top IB in the presence (and absence) of 120 μg/mL CFP pre-treatment. Fig. 5C shows that Top IB was capable of relaxing supercoiled DNA in the untreated-HepG2 cells when the amount of Top IB varied from 1.25 μg to 5 μg. The band of supercoiled DNA was observed when using 0.6 μg Top IB enzyme in the absence (or presence) of CFP extract might be due to too low Top IB activity needed to relax certain supercoiled DNA (Fig. 5C). When HepG2 cells was pretreated with 120 μg/mL CFP, supercoiled DNA was observed at 0.6 and 1.25 μg of Top IB (Fig. 5C). Top IB at 2.5 and 5 μg might be too high to be inhibited by cellular components released by CFP pretreated HepG2 cells. This result strongly indicates that there was a cellular effect from HepG2 cells after pretreatment with 120 μg/mL CFP, leading to inhibition of DNA relaxation. The present study indicates that CFP indirectly inhibited the activity of Top IB enzyme on DNA relaxation.

3.10. Anticancer effect in resistant HepG2 cells

One limitation of an ineffective liver cancer treatment is the generation of a resistance mechanism in liver cancer cells. Finding new anticancer agents that are sensitive in the resistant cancer cells is, therefore, of interest. In this study, the effect of CFP extract was tested in a cisplatin-resistant HepG2 cell line that has increasing MRP-1 activity and P-gp ABC efflux transporters (Junhom et al., 2016). CFP extract exerted a cytotoxic effect against resistant HepG2 cells with a higher IC_{50} value than the parental HepG2 cells ($IC_{50} = 196.7 \pm 18.1$ μg/mL; Fig. 6A); moreover, 500 μg/mL CFP induced 40% apoptosis cell death in resistant cells (not significantly different from the parental HepG2 cells after 24 h) (Fig. 6B). To confirm the cell death pathway, the expression of the respective pro-apoptotic (Bax) and anti-apoptotic proteins (Bcl-2) were also investigated. CFP extract at 500 μg/mL increased the expression level of Bax and decreased the expression level of Bcl-2 (Fig. 6C). It was, therefore, confirmed that CFP extract is a good candidate for new sources of anticancer agent; able to eliminate resistant cancer cells via apoptosis induction.

4. Discussion

The CFP extract was cytotoxic to HepG2 cells and induced the apoptotic death mode. Xanthones are a major group of compounds in the CFP extract and may have contributed to the apoptotic effect. Previous studies have suggested the higher cytotoxic potential of whole crude extract over its fraction or pure compound (Weerapreeyakul et al., 2016); due to a synergistic effect of compounds in the whole crude extract while masking any undesirable effect of the potent compound. FTIR microspectroscopy confirmed the change of biomolecules in HepG2 cells depending on the CFP extract. The result suggests a similar cellular effect of biochemical alteration and mechanisms of anticancer action of CFP and melphalan. The shift of the secondary protein structure from the α-helix to a β-pleated sheet was predominantly displayed in the amide I band contour with a best-fit of HepG2 treated with CFP extract and melphalan. This conformational alteration from an α-helix to a β-pleated sheet of amide I peak is known to be associated with caspase activation during apoptotic cell death (Lavrik et al., 2005). High lipid content in apoptotic cells can be used to distinguish apoptotic from necrotic cells whose plasma integrity is lost, leading to a low lipid component and a decrease in the FTIR signal of lipid region (Plaimee et al., 2014). It is postulated that high lipid content in apoptotic cells is due to the flip-flop of phosphatidylserine from inside to outside of the transmembrane protein (Plaimee et al., 2014). Basically, apoptotic cells undergo DNA degradation and DNA condensation resulting in low IR absorption in the nucleic region, while necrotic cells in which the DNA is degraded but not compacted will have a high IR absorption in the nucleic region (Plaimee et al., 2014; Junhom et al., 2016). High nucleic acid content was observed in both HepG2 cells treated with CFP extract or melphalan than the untreated cells; however, the percentage of necrotic cells was remarkably low although the concentration of CFP extract was increased. It was thus confirmed that CFP exerted another mechanism of anticancer action than an apoptosis inducing effect.

In cells undergoing apoptosis, the caspase enzymes are activated thereby triggering several proteolytic signals which amplify the signaling of apoptosis. Apoptosis induced by CFP extract was via both extrinsic and intrinsic pathways as evidenced from an increase in the activity of caspases 3, 8, and 9. The imbalance between pro-apoptotic (Bax) and anti-apoptotic proteins (Bcl-2) is related to mitochondrial (intrinsic) pathway induction in cells treated with CFP. The intrinsic apoptosis induction of CFP leads to mitochondrial membrane permeabilization and mitochondrial membrane potential (MMP) changes as reported previously (Nonpunya et al., 2014). The activation of caspase 9 is further downstream resulting in activation of caspase 3.

One of the effective death receptors related to apoptosis—with no effect against normal cells—is the tumor-necrosis-factor-related apoptosis-inducing ligand receptor (TRAILR). Normally, TRAIL induces apoptosis upon binding to TRAILR1 (death receptor 4; DR4) or TRAILR2 (death

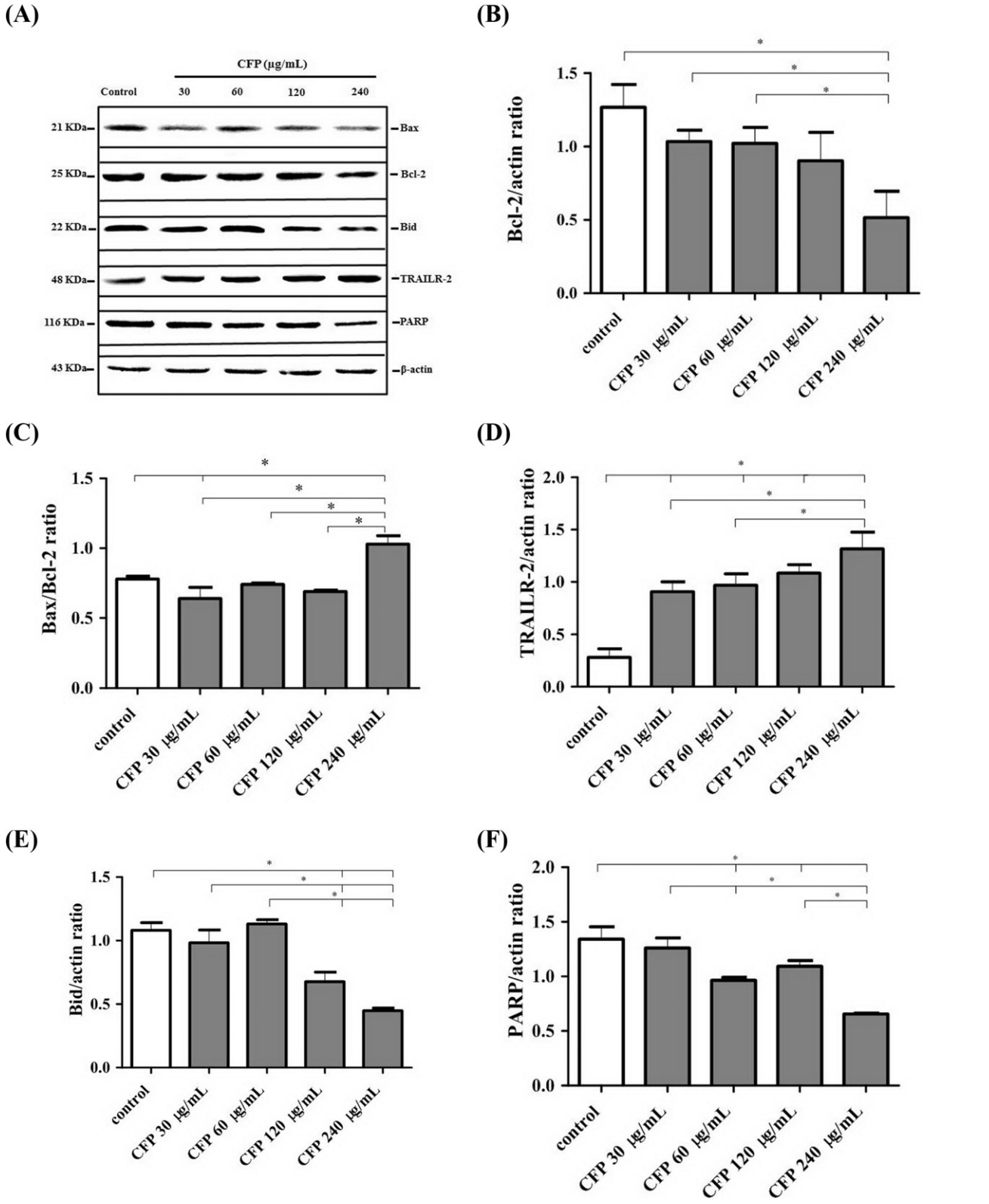

Fig. 4. Effects of CFP extract on expression of various death signals involved in apoptosis. HepG2 cells were treated with CFP extract at various concentrations (30, 60, 120, and 240 μg/mL) for 24 h. **(A)** Representative western blot of Bax, Bcl-2, TRAILR2, Bid, poly ADP ribose polymerase (PARP) protein expression after cells being treated with CFP compared to control and **(B–F)** expression levels of each proteins. Level of each protein was normalized to beta-actin. Results are from 3 independent experiments and presented as means ± standard deviation. *Statistically significant differences (mean ± SD, N = 3, one-way ANOVA followed by Tukey test, $P < 0.05$).

receptor 5; DR5), leading to Death Inducing Signaling Complex (DISC) formation. Then DISC auto-activates pro-caspase 8 enzyme followed by downstream activation of effector caspase 3 (McIlwain et al., 2013).

In the current study, it was found that the increasing caspase 8 activity caused by CFP was, moreover, triggered through the death-receptor pathway; based on the significantly up-regulated death receptor

Table 3
Alkylating activity and alkylating classification of CFP extracts and melphalan.

Samples	Absorbance $\lambda_{max} = 600$ nm	Alkylation classification
Melphalan	2.768	Abs > 0.50
CFP extract	1.137	(very high alkylating activity)
5-FU	0.144	Abs < 0.15
		(low alkylating activity)

TRAILR-2 at low concentration of CFP when compared to control group. In addition, caspase 8 also activated the mitochondrial pathway through cleavages of Bid. Bid protein has an important role in the crosstalk phenomena, which explains the coordination between the extrinsic and intrinsic pathways (Zhang et al., 2016). After cleavage, the cleaved Bid or truncated Bid (tBid) translocates to the outer membrane of the mitochondria, binds and activates oligomerization of the pro-apoptotic proteins (Bax and Bak), resulting in MMP changes followed by as release of

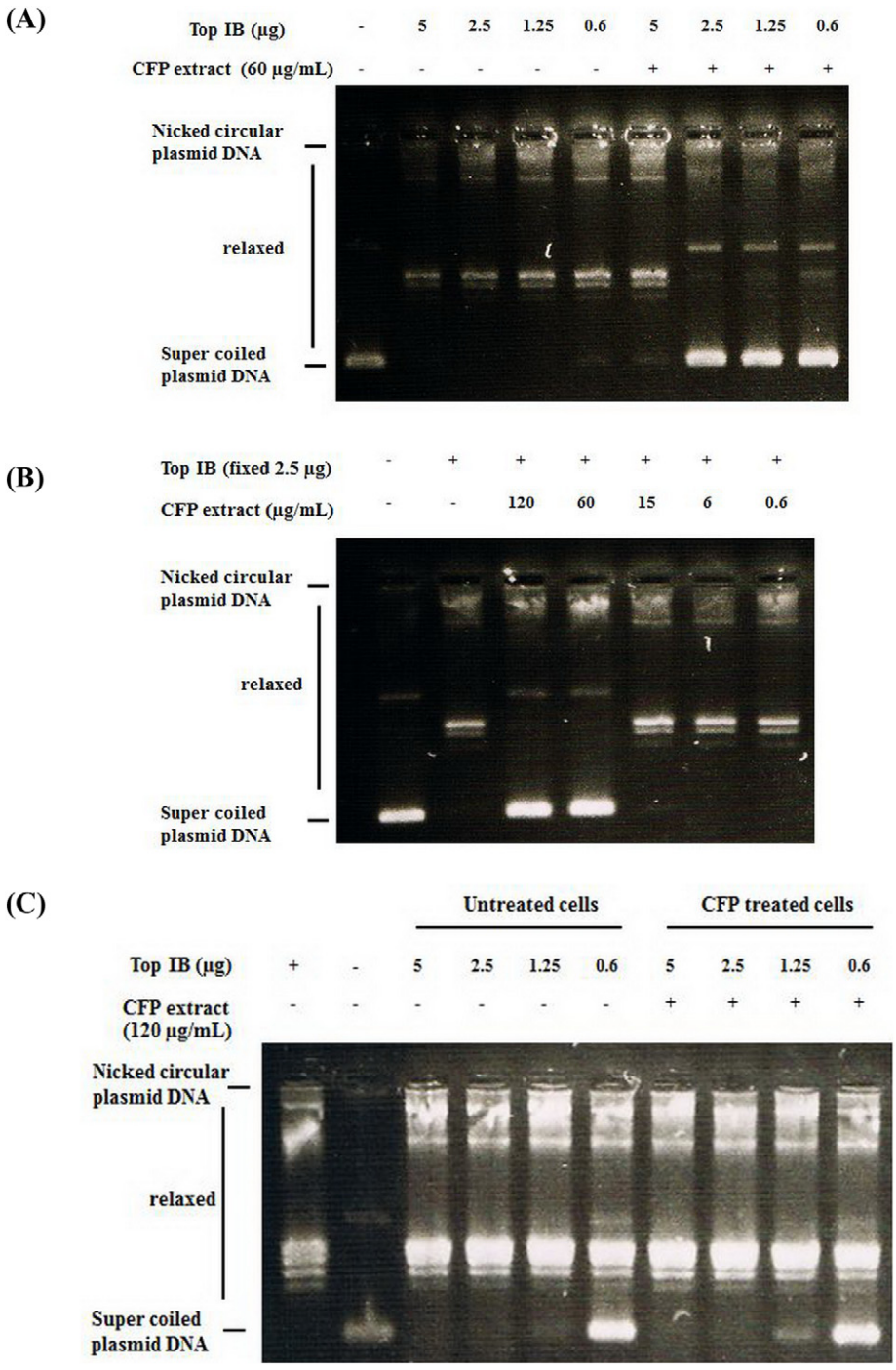

Fig. 5. Relaxation of negative supercoiled plasmid DNA by topoisomerase IB (Top IB). Direct inhibitory effect of CFP extract on TopIB enzyme on DNA relaxation. **(A)** Top IB content was varied from 0.6, 1.25, 5, to 2.5 μg, while CFP extract concentration was fixed at 60 μg/mL. **(B)** CFP extract concentration was varied when Top IB content was fixed at 2.5 μg. **(C)** Indirect relaxation effect was determined in the HepG2 cells after exposed to 120 μg/mL CFP extract for 1 h, while content of purified Top IB was varied. Reaction products were analyzed using agarose gel electrophoresis and visualized using nicked circular plasmid DNA and supercoiled plasmid DNA with ethidium bromide.

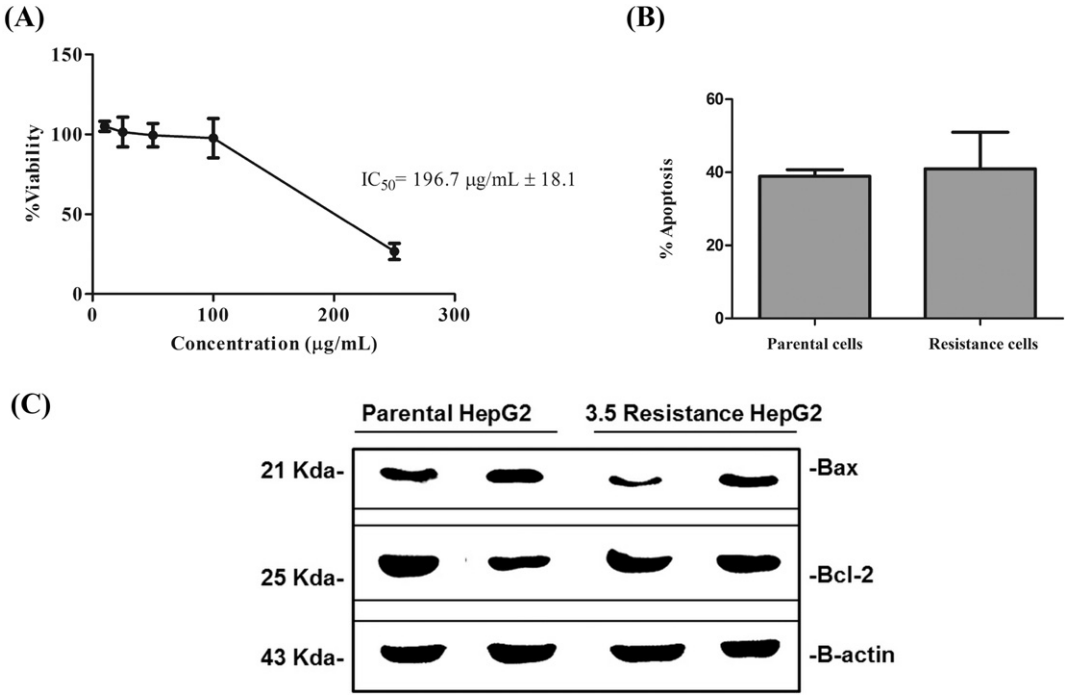

Fig. 6. Anticancer activity of CFP extract in the resistant HepG2 cell line at 24 h. **(A)** Cytotoxicity profile, **(B)** percentage of total apoptosis after treated with 2 × IC_{50} concentration (500 μg/mL) using flow cytometry, and **(C)** expression of pro-apoptotic protein (Bax) and anti-apoptotic protein (Bcl-2) after treated with 2 × IC_{50} concentration of CFP and determined using western blot analysis. Data represent 3 individual experiments. β-Actin was used in western blot analysis as an internal control for normalizing the increase/ decrease protein levels. CFP expression of pro-apoptotic protein (Bax) and anti-apoptotic protein (Bcl-2) CFP at 2 × IC_{50} concentration (500 μg/mL) by western blot analysis. The data represent in 3 individual experiments.

apoptogenic substances into cytosol and triggering the intrinsic apoptosis induction pathway (Tan et al., 2016). In the present study, the decrease expression of Bid protein was detected indicating the transformation into tBid followed by activation of apoptosis from the extrinsic toward the intrinsic pathway. This was evident from the study as demonstrated by the over-expressing of the TRAILR2 receptor after treatment with CFP, leading to increasing caspase 8 activation, and activation of Bid to crosstalk through the intrinsic pathway. The apoptosis signal was amplified through activation of pro-apoptotic proteins (i.e., Bax), which agrees with a previous report on CFP extract causing mitochondrial membrane alteration and release of cytochrome c (Nonpunya et al., 2014); caspase 9 activity was elevated followed by activation of downstream effector caspase 3 activity. Due to the small amount of CFP extract used to induce the extrinsic pathway, CFP seemed to preferably induce the apoptosis extrinsic pathway then cross-talked to the intrinsic pathway. A high concentration of the CFP extract and longer exposure to the HepG2 cells may be required in order to cause DNA damage after alkylation followed by damage to the mitochondria before induction of the apoptosis intrinsic pathway.

During apoptosis, the activated caspase 3 will cleave several intracellular targets including the poly ADP-ribose polymerase (PARP) enzyme and DNA topoisomerase I (Top I) (Vizetto-Duarte et al., 2016). Topoisomerases (Top) can either cleave one strand of the DNA duplex or pass the intact complementary strand through the nick (type I topoisomerase), or cleave both strands and pass an intact duplex segment through the double-strand break (type II topoisomerase). Type I enzymes are classified into the IA, IB, and IC families (Pommier et al., 2010). Top IB is classified as a eukaryotic DNA topoisomerase. It relaxes DNA that has been supercoiled by forming a covalent bond for breaking and rejoining at the 3′ end of the cleaved DNA strand. Topoisomerase I (Top I) is known to relax DNA supercoiling, which is generated during transcription, replication, and chromatin remodeling (Xu and Her, 2015).

Inhibition of the Top IB enzyme can protect the supercoiled DNA from relaxation, which can be observed using the relaxation assay (Seol et al., 2015). Previously, CFP was reported to induce apoptosis induction by causing DNA fragmentation (Nonpunya et al., 2014). The current study showed that CFP exerted strong alkylating action and significantly decreased the expression of full-length PARP (116 KDa), which is involved in DNA repair.

PARP is responsible for driving the biological process and is associated with several DNA repair pathways (e.g., base excision repair for maintenance of genome interiority) (Tan et al., 2016; Zhang et al., 2016). The presence of PARP indicates DNA single strand breaks (SSB). PARP binds to the damaged DNA via its N-terminal zinc finger motifs. The rapid binding of PARP to DNA SSB is critical for not only eliminating the effect of the alkylating agent but also for reversing the activity of the Top IB inhibitor that causes topo poisoning (Murai et al., 2014). The decreasing or inhibiting of PARP activity is, therefore, necessary for a new strategy of cancer therapy due to the inhibition of the repair process. In the current study, it is evident that CFP extract triggered apoptosis by generating caspase 3 activity, which inactivated PARP function (i.e., the PARP cleavage form), so that DNA damage could not be repaired. Ultimately, apoptosis cell death occurred.

Alkylation is an effective anticancer mechanism that can trigger DNA SSB due to its ability to alkylate methyl or alkyl groups into the DNA strand (Zhou et al., 2016). CFP extract acts as a strong alkylating agent, so it could damage DNA and cause DNA strand breaks. Since PARP is also inhibited by CFP extract, the DNA repair process could be halted. CFP extract, moreover, directly and indirectly inhibits Top IB activity, preventing the DNA relaxation process so it may also potentiate DNA strand breaks which cannot be repaired.

Topoisomerase I (Top I) enzyme is important for releasing the torsion in the DNA strand during the replication or transcription process (Xu and Her, 2015). Top I relaxes supercoiled DNA through a breakage/rejoining reaction by forming a covalent bond with the 3′ end of the cleaved DNA strand, yielding the topoisomerase I cleavage complex (Top 1CC) or Topo poison. Top inhibition—by stabilizing the Top 1CC—leads to DNA uncoiling and increasing DNA strand breaks (Xu and Her, 2015). Top 1CC can, however, be reversed through a repair mechanism; particularly PARP activation in cancer cells that makes cancers resistant to Top I inhibitors (Xu and Her, 2015). It has been reported that PARP inhibitors enhance the effect of Top I inhibitors both in vitro

and in vivo (Patel et al., 2016). In order to overcome the resistance mechanism, compounds which block not only Top I but also the PARP enzyme would be good anticancer candidates.

5. Conclusion

The present study offers an in-depth looks at the cellular mechanisms of the anticancer action of CFP extract from *C. formosum* ssp. *pruniflorum*. CFP extract is potentially a source of anticancer agents, which may work in synergy or through a multi-targeted mechanism. The safe systemic use of CFP is possible according to its traditional used with high selectivity to cancer targeted cells. Further study might focus on the in vivo pharmacokinetics of CFP in animals.

Disclosure of interest

The authors declare that they have no conflict of interest.

Acknowledgments

AN was supported by the Research Fund for Supporting Lecturers to Admit High Potential Students to Study and Research in her Expert Program Year 2010, Khon Kaen University and the Erasmus Mundus project TECHNO I – 3rd cohort for the scholarship for study and research exchange to European Universities scholarship, Rome Tor Vergata University, Rome, Italy, 2014. The authors thank (a) the Plant Genetics Conservation Project under the Royal Initiation of Her Royal Highness Princess Maha Chakri Sirindhorn for the permission of conducting research, (b) Professor Alessandro Desideri for providing the purified topoisomerase IB (Top IB) enzyme and useful discussion, (c) Dr. Cholpajsorn Junhom for laboratory assistance, and (d) Mr. Bryan Roderick Hamman for assistance with the English-language presentation of the manuscript.

References

Anderson, E.F., 1986. Ethnobotany of hill tribes of Northern Thailand. II. Lahu medicinal plants. Economic Botany 40, 442–450.

Boonnak, N., Karalai, C., Chantrapromma, S., Ponglimanont, C., Fun, H-K., Kanjana-Opas, A., Laphookhieo, S., 2006. Bioactive prenylated xanthones and anthraquinones from *Cratoxylum formosum* ssp. *pruniflorum*. Tetrahedron 62, 8850–8859.

Boonnak, N., Karalai, C., Chantrapromma, S., Ponglimanont, C., Kanjana-Opas, A., Chantrapromma, K., Kato, S., 2010. Chromene and prenylated xanthones from the roots of *Cratoxylum formosum* ssp. *pruniflorum*. Chemical and Pharmaceutical Bulletin 58, 386–389.

Boonnak, N., Chantrapromma, S., Tewtrakul, S., Sudsai, T., 2014. Inhibition of nitric oxide production in lipopolysaccharide-activated RAW264.7 macrophages by isolated xanthones from the roots of *Cratoxylum formosum* ssp. *pruniflorum*. Archives of Pharmacal Research 37, 1329–1335.

Boonsri, S., Karalai, C., Ponglimanont, C., Kanjana-opas, A., Chantrapromma, K., 2006. Antibacterial and cytotoxic xanthones from the roots of *Cratoxylum formosum*. Phytochemistry 67, 723–727.

Budzisz, E., Brzezinska, E., Krajewska, U., Rozalski, M., 2003. Cytotoxic effects, alkylating properties and molecular modeling of coumarin derivatives and their phosphonic analogues. European Journal of Medicinal Chemistry 38, 597–603.

Duan, Y.-H., Dai, Y., Wang, G.-H., Zhang, X., Chen, H.-F., Chen, J.-B., Yao, X.-S., Zhang, X.-K., 2010. Bioactive xanthones from the stems of Cratoxylum formosum ssp. pruniflorum. Journal of Natural Products 73, 1283–1287.

Duan, Y.-H., Dai, Y., Wang, G.-H., Chen, H.-F., Gao, H., Chen, J.-B., Yao, X.-S., Zhang, X.-K., 2011. Xanthone and benzophenone glycosides from the stems of Cratoxylum formosum ssp. pruniflorumChemical and Pharmaceutical Bulletin 59, 231–234.

Gangwar, M., Gautam, M.K., Sharma, A.K., Tripathi, Y.B., Goel, R.K., Nath, G., 2014. Antioxidant capacity and radical scavenging effect of polyphenol rich *Mallotus philippenensis* fruit extract on human erythrocytes: an in vitro study. The Scientific World Journal 2014, 279451.

Grosvenor, P.W., Gothard, P.K., McWilliam, N.C., Supriono, A., Gray, D.O., 1995a. Medicinal plants from Riau province, Sumatra, Indonesia. Part 1: uses. Journal of Ethnopharmacology 45, 75–95.

Grosvenor, P.W., Supriono, A., Gray, D.O., 1995b. Medicinal plants from Riau province, Sumatra, Indonesia. Part 2: antibacterial and antifungal activity. Journal of Ethnopharmacology 45, 97–111.

Issara-Amphorn, J., T-Thienprasert, N.P., 2014. Preliminary in vitro pro-apoptotic effects of *Cratoxylum formosum* crude leaf extracts. International Journal of Applied Research in Natural Products 7, 26–30.

Jahan, Z., Castelli, S., Aversa, G., Rufini, S., Desideri, A., Giovanetti, A., 2013. Role of human topoisomerase IB on ionizing radiation induced damage. Biochemical and Biophysical Research Communications 432, 545–548.

Junhom, C., Weerapreeyakul, N., Tanthanuch, W., Thumanu, K., 2016. FTIR microspectroscopy defines early drug resistant human hepatocellular carcinoma (HepG2) cells. Experimental Cell Research 340, 71–80.

Keowkase, R., Weerapreeyakul, N., 2016. *Cratoxylum formosum* extract protects against amyloid-beta toxicity in a *Caenorhabditis elegans* model of Alzheimer's disease. Planta Medica 82, 516–523.

Kuete, V., Wabo, H.K., Eyong, K.O., Feussi, M.T., Wiench, B., Krusche, B., Tane, P., Folefoc, G.N., Efferth, T., 2011. Anticancer activities of six selected natural compounds of some Cameroonian medicinal plants. PLoS One 6, e21762.

Kukongviriyapan, U., Luangaram, S., Leekhaosoong, K., Kukongviriyapan, V., Preeprame, S., 2007. Antioxidant and vascular protective activities of *Cratoxylum formosum*, *Syzygium gratum* and *Limnophila aromatica*. Biological and Pharmaceutical Bulletin 30, 661–666.

Kuvatanasuchati, J., Laphookhieo, S., Rodanant, P., 2011. Antimicrobial activity against periodontopathic bacteria and cytotoxic study of *Cratoxylum formosum* and *Clausena lansium*. Journal of Medicinal Plant Research 5, 5988–5992.

Lavrik, I.N., Golks, A., Krammer, P.H., 2005. Caspases: pharmacological manipulation of cell death. Journal of Clinical Investigation 115, 2665–2672.

Lowry, O.H., Rosebrough, N.J., Farr, A.L., Randall, R.J., 1951. Protein measurement with the Folin phenol reagent. The Journal of Biological Chemistry 193, 265–275.

Machana, S., Weerapreeyakul, N., Barusrux, S., Thumanu, K., Tanthanuch, W., 2012. FTIR microspectroscopy discriminates anticancer action on human leukemic cells by extracts of *Pinus kesiya*; *Cratoxylum formosum* ssp. *pruniflorum* and melphalan. Talanta 93, 371–382.

Maisuthisakul, P., Pongsawatmanit, R., Gordon, M.H., 2006. Antioxidant properties of Teaw (*Cratoxylum formosum* Dyer) extract in soybean oil and emulsions. Journal of Agricultural and Food Chemistry 54, 2719–2725.

Manosroi, J., Boonpisuttinant, K., Manosroi, W., Manosroi, A., 2012. Anti-proliferative activities on HeLa cancer cell line of Thai medicinal plant recipes selected from MANOSROI II database. Journal of Ethnopharmacology 142, 422–431.

McIlwain, D.R., Berger, T., Mak, T.W., 2013. Caspase functions in cell death and disease. Cold Spring Harbor Perspectives in Biology 5, a008656.

Murai, J., Huang, S.Y., Renaud, A., Zhang, Y., Ji, J., Takeda, S., Pommier, Y., 2014. Stereospecific PARP trapping by BMN 673 and comparison with Olaparib and Rucaparib. Molecular Cancer Therapeutics 13, 433–443.

Nonpunya, A., Weerapreeyakul, N., Barusrux, S., 2014. *Cratoxylum formosum* (Jack) Dyer ssp. *pruniflorum* (Kurz) Gogel. (Hóng yá mù) extract induces apoptosis in human hepatocellular carcinoma HepG2 cells through caspase-dependent pathways. Chinese Medicine 9, 12.

Patel, A.G., Flatten, K.S., Peterson, K.L., Beito, T.G., Schneider, P.A., Perkins, A.L., Kaufmann, S.H., 2016. Immunodetection of human topoisomerase I-DNA covalent complexes. Nucleic Acids Research 44, 2816–2826.

Plaimee, P., Weerapreeyakul, N., Thumanu, K., Tanthanuch, W., Barusrux, S., 2014. Melatonin induces apoptosis through biomolecular changes, in SK-LU-1 human lung adenocarcinoma cells. Cell Proliferation 47, 564–577.

Pommier, Y., Leo, E., Zhang, H., Marchand, C., 2010. DNA topoisomerases and their poisoning by anticancer and antibacterial drugs. Chemistry and Biology 17, 421–433.

Prayong, P., Barusrux, S., Weerapreeyakul, N., 2008. Cytotoxic activity screening of some indigenous Thai plants. Fitoterapia 79, 598–601.

Seol, Y., Zhang, H., Agama, K., Lorence, N., Pommier, Y., Neuman, K.C., 2015. Single-molecule supercoil relaxation assay as a screening tool to determine the mechanism and efficacy of human topoisomerase IB inhibitors. Molecular Cancer Therapeutics 14, 2552–2559.

Siriwarin, B., Weerapreeyakul, N., 2016. Sesamol induced apoptotic effect in lung adenocarcinoma cells through both intrinsic and extrinsic pathways. Chemico-Biological Interactions 254, 109–116.

Sripanidkulchai, K., Teepsawang, S., Sripanidkulchai, B., 2010. Protective effect of *Cratoxylum formosum* extract against acid/alcohol-induced gastric mucosal damage in rats. Journal of Medicinal Food 13, 1097–1103.

Srisayam, M., Weerapreeyakul, N., Barusrux, S., Tanthanuch, W., Thumanu, K., 2014. Application of FTIR microspectroscopy for characterization of biomolecular changes in human melanoma cells treated by sesamol and kojic acid. Journal of Dermatological Science 73, 241–250.

Tan, C.T, Zhou, Q.-L., Su, Y.-C., Fu, N.Y, Chang, H.-C, Tao, R.N, Sukumaran, S.K, Baksh, S., Tan, Y.-J., Sabapathy, K., Yu, C.-D, Yu, V.C., 2016. MOAP-1 mediates Fas-induced apoptosis in liver by facilitating tBid recruitment to mitochondria. Cell Reports 16, 174–185.

Ukoha, P.O., Cemaluk, E.A.C., Nnamdi, O.L., Madus, E.P., 2011. Tannins and other phytochemical of the *Samanaea saman* pods and their antimicrobial activities. African Journal of Pure and Applied Chemistry 5, 237–244.

Vizetto-Duarte, C., Custódio, L., Gangadhar, K.N., Lago, J.H., Dias, C., Matos, A.M., Neng, N., Nogueira, J.M., Barreira, L., Albericio, F., Rauter, A.P., Varela, J., 2016. Isololiolide, a carotenoid metabolite isolated from the brown alga *Cystoseira tamariscifolia*, is cytotoxic and able to induce apoptosis in hepatocarcinoma cells through caspase-3 activation, decreased Bcl-2 levels, increased p53 expression and PARP cleavage. Phytomedicine 23, 550–557.

Waiyaput, W., Payungporn, S., Issara-Amphorn, J., Panjaworayan, N.T.T., 2012. Inhibitory effects of crude extracts from some edible Thai plants against replication of hepatitis B virus and human liver cancer cells. BMC Complementary and Alternative Medicine 12, 246.

Weerapreeyakul, N., Machana, S., Barusrux, S., 2016. Synergistic effects of melphalan and *Pinus kesiya* Royle ex Gordon (Simaosong) extracts on apoptosis induction in human cancer cells. Chinese Medicine 11, 29.

Xiong, J., Liu, X.-H., Bui, V.-B., Hong, Z.-L., Wang, L.-J., Zhao, Y., Fan, H., Yang, G.-X., Hu, J.-F., 2014. Phenolic constituents from the leaves of *Cratoxylum formosum* ssp. *pruniflorum*. Fitoterapia 94, 114–119.

Xu, Y., Her, C., 2015. Inhibition of topoisomerase (DNA) I (TOP1): DNA damage repair and anticancer therapy. Biomolecules 5, 1652–1670.

Zhang, F., Chen, L., Jin, H., Shao, J., Wu, L., Lu, Y., Zheng, S., 2016. Activation of Fas death receptor pathway and Bid in hepatocytes is involved in saikosaponin D induction of hepatotoxicity. Environmental Toxicology and Pharmacology 41, 8–13.

Zhou, Q., Ji, M., Zhou, J., Jin, J., Xue, N., Chen, J., Chen, X., 2016. Poly (ADP-ribose) polymerases inhibitor, Zj6413, as a potential therapeutic agent against breast cancer. Biochemical Pharmacology 107, 29–40.

Zhu, R.X., Seto, W.K., Lai, C.L., Yuen, M.F., 2016. Epidemiology of hepatocellular carcinoma in the Asia-Pacific region. Gut and Liver 10, 332–339.